Key Engineering Materials Vol. 287 (2005) pp. 421-426
online at http://www.scientific.net

Effect of Grain Boundary Phase on Contact Damage Resistance of Silicon Nitride Ceramics

Chul Seung Lee[1,a], Kee Sung Lee[2,b], Shiwoo Lee[3,c] and Do Kyung Kim[1,d]

[1]Dept. of Materials Science and Eng., KAIST, Daejeon, 305-701, Korea

[2]School of Mechanical and Automotive Eng., Kookmin University, Seoul, 136-702, Korea

[3]Energy Materials Research Center, Korea Institute of Energy Research, Daejeon, 305-345, Korea

[a]chulseung.lee@samsung.com, [b]keeslee@kookmin.ac.kr, [c]crater@kier.re.kr, [d]dkkim@kaist.ac.kr

Keywords : Silicon Nitride, Grain Boundary Phase, Sintering Additive, Hertzian Contact

Abstract. Contact damage resistances of silicon nitride ceramics with various grain boundary phases are investigated in this study. The grain boundary phases are controlled by the addition of different types of sintering additives, or the crystallization of intergranular phase in a silicon nitride. We control the microstructures of materials to have similar grain sizes and the same phases to each other. Contact testing with spherical indenters is used to characterize the damage response. The implication is that the grain boundary phase can be another controllable factor against contact damage and strength degradation even though it is not critical relative to the effect of grain morphology.

Introduction

Silicon nitride (Si_3N_4) ceramics have been studied with particular interest for several decades in high temperature applications such as burner nozzles, combustion and engine components because of high thermal shock resistance [1]. As Si_3N_4 ceramics has high wear resistance, it is also applicable for cutting tools and bearings [2]. A mechanical contact is one of the important characterizations to consider the lifetime of these components [3]. The surfaces of material can be subjected to contact loads, from single to multiple concentrated loads. The critical stresses can introduce localized damage and crack, which be a critical flaw to cause a catastrophic failure. Thus, reduced sensitivities against the damages – "flaw tolerance" or "damage tolerance" - produced by the contact stresses are required to prolong the lifetime of the components in service [4-7]. Hertzian indentation is a simple technique to induce contact damage on the flat surface. A hard spherical indenter is pressed on the surface of the specimen and ceramographic sectionings or bonded specimens are used to examine the damage patterns [8].

While Si_3N_4 ceramics exhibit excellent thermal and mechanical properties at both room temperature and high temperature, the critical drawback is low reliability due to inferior fracture toughness rather than a commercial metal. Many studies demonstrated that the mechanical properties of Si_3N_4 are influenced by a heterogeneous microstructure with weak grain boundary phases [9,10]. The microstructure of fine and equiaxed grains represents the failure behavior of brittle crack production. On the other hand, the microstructure including coarse and heterogeneous microstructure produce diffuse microcrack zones consisting of long and elongated grains, with enhanced fracture toughness as well as rising toughness curve in the long-crack domain due to grain bridging along with weak interfacial fracture [10].

Nevertheless, understanding of the microstructure effect on the contact resistance is still disputable, because of the complexity between such variables as grain size, aspect ratio, α/β phase ratio, and the composition of glassy secondary phase. These microstructural variables usually vary in an interdependent manner at the same sintering condition. Very recently, the effect of α/β phase on the contact resistance was differentiated from the grain morphology [11]. On the other hand, the effect of grain boundary phase is still arguable. It is valuable to elucidate the role of grain boundary

in the damage patterns because weak interphase boundaries and high local thermal expansion mismatch stresses can toughen the material locally by crack bridging mechanism.

In the present study we investigate the role of grain boundary phase on the contact resistance of Si_3N_4 ceramics. We prepared the different grain boundary composition by changing sintering additives, Al_2O_3+Y_2O_3 or MgO and sintering temperature to have the same grain size, aspect ratio and α/β phase. Then we characterize the damage accumulation by Hertzian indentation with sphere indenters. We also investigate the role of crystallization in the grain boundary phase of silicon nitride ceramics upon the contact resistance. Distinction between damages related with the grain boundary mismatch will be discussed in this study.

Experimental procedure

A common powder processing and firing procedure was used for preparing Si_3N_4 materials with different grain boundary phases. The starting silicon nitride powers investigated in this study were fine α-Si_3N_4 (UBE-SN-E10, Ube Industries, Tokyo, Japan). Sintering additives were 6 wt% Y_2O_3 (Fine Grade, H. C. Starck GmbH, Goslar, Germany) and 2 wt% Al_2O_3 (AKP 50, Sumitomo Chemical Co. Ltd., Tokyo, Japan), or 6.24 wt% (5.6vol%) MgO (Kokusan Chemical Works Ltd., Tokyo, Japan). The other set of sintering additives for crystallization were 5 wt% Y_2O_3 (Fine Grade, H. C. Starck GmbH, Goslar, Germany), 2 wt% Al_2O_3 (AKP 50, Sumitomo Chemical Co. Ltd., Tokyo, Japan), and 1 wt% MgO (Kokusan Chemical Works Ltd., Tokyo, Japan).

The powders were mixed in isopropanol for 24 h in a planetary ball mill, using zirconia balls in a propylene container. After drying, the softly agglomerated powder was crushed and sieved through a 60-mesh screen. The powders were hot pressed in a graphite mold of 20mm diameter at various temperatures, to get similar microstructure, from 1700°C~1800°C for 1hr at a pressure of 25MPa in N_2 gas. Some of the specimens were post-sintered at 1450°C for 20 hr in N_2 gas to crystallize the glass phase on the grain boundary.

The disk sintered products were cut into bar specimen with dimensions of 15 mm × 4 mm × 3 mm. Specimen surfaces normal to the hot-press direction were grinded, and then polished to 1 μm finish. These surfaces were plasma etched to highlight the grain structures. After gold coating, the etched surfaces were examined by scanning electron microscopy (SEM), and grain sizes, shapes, and aspect ratio were determined using an image analyzer (OPTIMAS 4.0, Bioscan Inc., Edmonds, WA, U.S.A.). X-ray diffraction (XRD) was used to determine the α/β phase ratio for each material. Densities were measured using the Archimedes method.

Hertzian indentations were made with a WC sphere of radius r = 1.98mm (J&L Industrial Supply Co., MI, U.S.A.) at load P = 500 N ~ 3500 N on the surface. The indentations were made symmetrically along the traces of the interfaces on the top surfaces in the bonded-specimen at P = 3500 N. After separating the indented specimen halves in solvent, a gold coat was applied to the side surfaces for viewing in Nomarski contrast to observe the damage evolution.

Bar specimens were indented in air at the center of polished face using WC ball with a radius of 1.98mm at contact loads from P = 1500 N to 3500 N by universal testing machine. Indented specimens were broken in flexure with the polished sides in tension with a crosshead speed of 30mm/min using four-point support on a universal test machine. The strengths were calculated from beam theory, using the conventional relation

$$\sigma_F = 3Fl/4wd^2 \quad (1)$$

with l the moment span, w the bar width, d the sample thickness and F the breaking load. The bending tests follow the extension of contact damages by tensional stresses, σ. Some specimens were prepared without spherical indentations, for measurement of "laboratory" strengths. All broken specimens were also examined by optical microscopy to confirm the failure origin.

The glass compositions with Y-Si-Al-O-N or Mg-Si-O-N were prepared from the same powder processing and firing condition to analyze the residual stress in the glassy phase. The compositions

were selected within the G regions as shown in Fig.1. The sintered glass was cut into 3 x 3 x 9 mm and thermal expansion was measured using TMA (SETARAM 92-16/18) from room temperature to 1000°C. The residual stresses were calculated from thermal expansion mismatch [12].

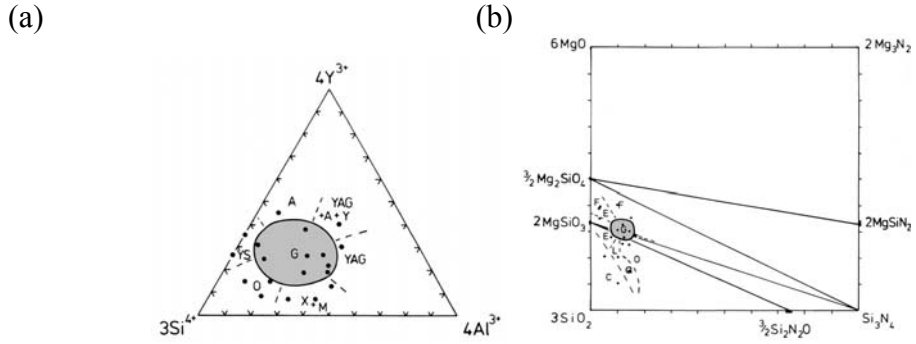

Fig. 1 – Phase diagrams of (a) Y-Si-Al-O-N system at 16equ% N. (b) Mg-Si-O-N system at 1700°C. Gray area is glass formation region. Composition G is selected for making glass.

Results and discussion

Figure 2 shows scanning electron microscopy (SEM) micrographs of the Si_3N_4 sintered by the addition of different sintering additives. In Fig. 2(a), the microstructure of Si_3N_4 with Y_2O_3 and Al_2O_3 additives was represented after hot pressing at 1750°C and plasma etching. The similar microstructure of the Si_3N_4 with MgO additive prepared at different sintering condition, 1700°C, was revealed in Fig. 1(b). These materials consist of mainly elongated β phases with minor α phases. Density measurements for two materials resulted in high relative density, >99%.

Figure 3 shows the SEM micrographs of the Si_3N_4 microstructures without the crystallization (Fig.1(a)) and with the crystallization (Fig. 1(b)). Porosity is not evident in two plasma-etched specimens and density measurement confirmed full density (>99%) using Archimedes method. The microstructure contains elongated β grains. There is no distinct discrepancy on the microstructure before and after the crystallization.

The result of microstructure analysis using an image analyzer was summarized in Table 1. The α/β phase fraction, average grain size, and aspect ratio are controlled to have a similar microstructure to each other in order to investigate the role of only grain boundary composition within the microstructure on the contact resistance.

Table 1 – Microstructural characterization of Si_3N_4 ceramics with different grain boundary phases.

Characterisitcs	Si_3N_4 with different additive		Si_3N_4 with different phase	
	$Al_2O_3 + Y_2O_3$	MgO	glassy	crystalline
mean grain size (μm)	0.23 ± 0.14	0.27 ± 0.16	0.23 ± 0.21	0.25 ± 0.18
aspect ratio	5.30 ± 1.52	5.71 ± 1.99	5.23 ± 1.47	5.30 ± 1.46
β/α phase ratio	0.67	0.686	1.00	1.00
relative density (%)	> 99	> 99	> 99	> 99

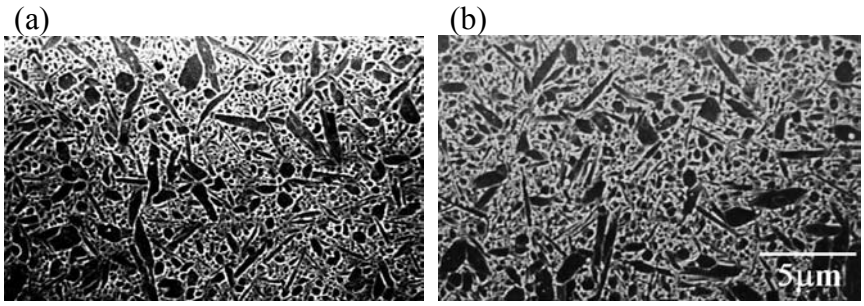

Fig. 2 – SEM micrographs of Si_3N_4 sintered by the addition of (a) Y_2O_3+Al_2O_3 additive and (b) MgO additive.

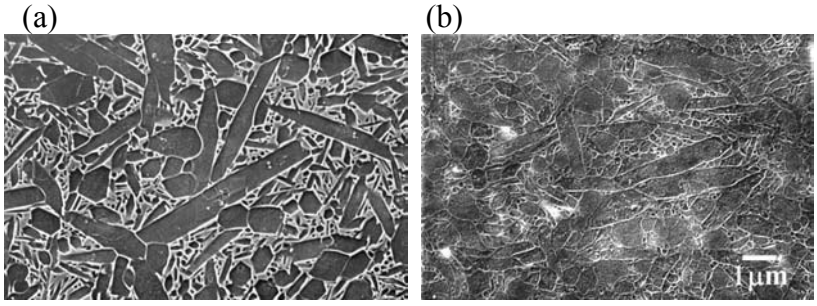

Fig. 3 – SEM micrographs of Si_3N_4 sintered by the addition of the same additive; (a) before and (b) after crystallization.

Figure 4 illustrate contact fracture in Si_3N_4 materials with different sintering additives, formed at a relatively high load, P = 3500 N. The cone crack is substantially shallower and the quasi-plasticity zone is more intense in the subsurface of the Si_3N_4 with Al_2O_3 and Y_2O_3 additives in Fig. 4(a). On the other hand, a classical cone crack is well developed outside the contact, indicative of brittleness, and signs of minor quasi-plasticity in the Si_3N_4 with MgO additive as shown in Fig. 4(b). Serial surface observation after spherical indentation confirmed that the initiation load of cone crack for the Si_3N_4 with MgO additive is slightly lower, P_c = 2100 N, rather than one with Y_2O_3 and Al_2O_3 additives, P_c = 2400 N. It is apparent that changing of grain boundary composition greatly affects contact damage and crack initiation load. Therefore, one of the important microstructural elements is the composition at grain boundaries by changing of sintering additives in the starting powder.

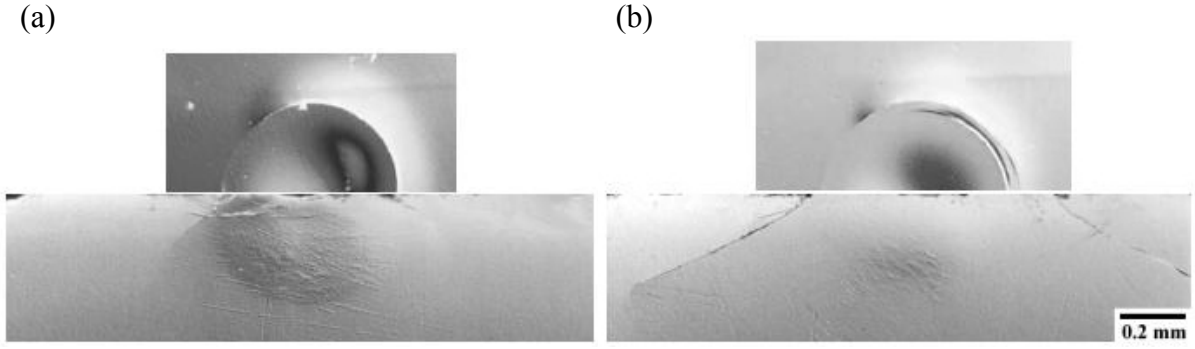

Fig. 4 – Contact fracture in Si_3N_4 with the additive of (a) Al_2O_3+Y_2O_3 and (b) MgO, using WC sphere r = 1.98mm at P = 3500 N, showing half-surface (upper) and side (lower) views.

Figure 5 compares the bonded-interface section views, including contact damages produced in the Si_3N_4 with and without crystallization from indentation using a WC ball with a radius of 1.98

mm at a relatively high load, P = 3500 N. The Si_3N_4 without crystallization shows relative damage tolerance by the conspicuous formation of quasi-plasticity zone. The damage absorption in this quasi-plasticity damage zone brings relatively high tolerance against the initiation of cone crack from the surface. Serial surface observation after spherical indentation confirmed that the initiation load of cone crack for the Si_3N_4 without crystallization is slightly higher, P_c = 2700 N, rather than crystallization, P_c = 2400 N.

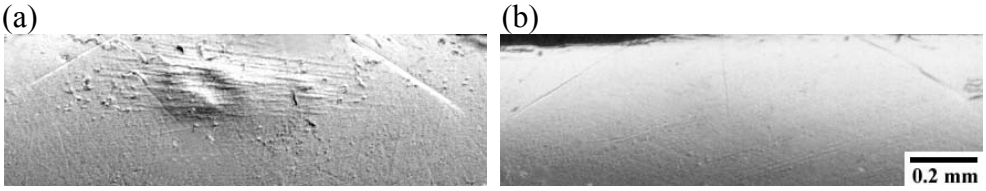

Fig. 5 – Contact fracture in Si_3N_4 with (a) glassy phase boundary and (b) crystalline phase boundary, using WC sphere r = 1.98mm at P = 3500 N, showing side views.

Experimental data for the strength of Si_3N_4 with different grain boundary phases as a function of contact load are plotted in Fig. 6. As the P_c of the Si_3N_4 with Al_2O_3 and Y_2O_3 is slightly higher, the strength falloff occurs at slightly higher load as shown in Fig. 6(a). The point of strength falloff relatively shifts upward at the Si_3N_4 with glassy boundaries in Fig. 6(b). While there are no significant strength degradations at $P < P_c$, abrupt strength reductions occur at P_c. At the contact load exceeding the cone crack initiation load, $P > P_c$, strength value abruptly falloff, with failures from cone cracks. The strength is determined from the Griffith strength relation and consideration of the cone crack geometry,

$$\sigma_F = T_o / c^{1/2} \tag{2}$$

with cone crack length c.

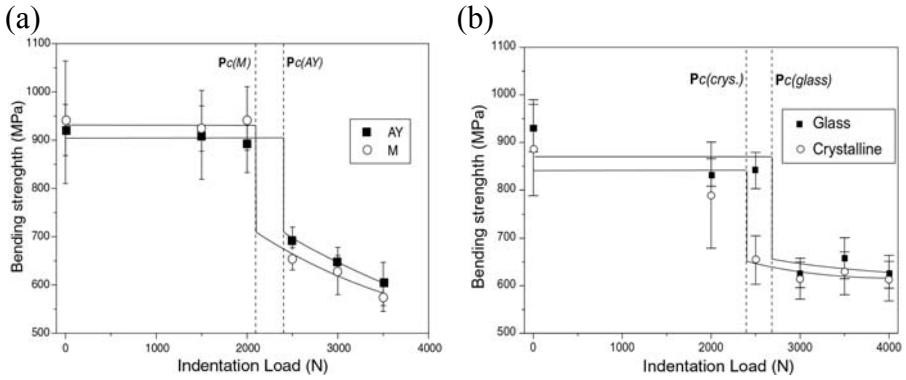

Fig. 6 – Strength degradations of Si_3N_4 with different phase boundaries, (a) by Y_2O_3+Al_2O_3 (AY) or MgO(M) additives and (b) by glassy or crysalline phases, for contacts with WC sphere radius r = 1.98 mm. Data plotted as a function of indentation load P.

The residual stresses in Si_3N_4 grain and glassy boundaries calculated from thermal expansion were plotted as shown in Fig. 7. Higher residual tension stress at the grain boundaries for the Si_3N_4 with Al_2O_3 and Y_2O_3 additives easily creates microcracks in the subsurface during the contact by shear stress at yield zone of distributed shear-driven faults. Therefore, it is thought that the deformation zone including shear faults and microcracks inevitably absorbs mechanical energy, and delays slightly the cone crack initiation from the surface. Likewise, it is conjectured that relative lower toughness of glassy boundary relative to crystalline boundary creates microcracks easily

under the same load, which lead to delayed strength falloff.

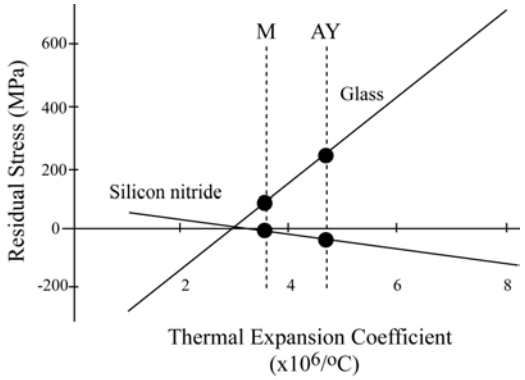

Fig. 7 – Calculated residual stresses induced in MgO added Si_3N_4 (M) and Y_2O_3+Al_2O_3 added Si_3N_4 (AY).

Summary

The role of grain boundary phase on contact damage behavior in silicon nitride ceramics was investigated using Hertzian indentation test. In order to consider only grain boundary effect, all of the microstructure effect except grain boundary was fixed. Grain boundary phase were changed as two methods. One was changing grain boundary composition, and the other crystallization. As a result, the damage modes of Si_3N_4 with 6wt% Y_2O_3 and 2wt% Al_2O_3 showed slightly damage tolerant rather than Si_3N_4 with 6.24wt% MgO additive. The effect of crystallization on the grain boundary phase was found to result in slightly lower critical load of crack initiation on the surface.

References

[1] F. F. Lange: J. Am. Ceram. Soc. Vol. 59 (1973), p. 518

[2] C. Greskovich and G. E. Gazza: J. Mater. Sci. Lett. Vol. 4 (1985), p. 195

[3] B. R. Lawn: *Fracture of Brittle Solids* (Cambridge solid state science series, New York, USA 1975).

[4] K. S. Lee, S. K. Lee, B. R. Lawn and D. K. Kim: J. Am. Ceram. Soc. Vol. 81 (1998), p. 2394

[5] S. J. Bennison, N. P. Padture, J. L. Runyan and B. R. Lawn: Phil. Mag. Lett. Vol. 64 (1991), p. 191

[6] N. P. Padture, S. J. Bennison and H. M. Chan: J. Am. Ceram. Soc. Vol. 76 (1993), p. 2312

[7] S. K. Lee and B. R. Lawn: J. Am. Ceram. Soc. Vol. 81 (1998), p.997

[8] B. R. Lawn: J. Am. Ceram. Soc. Vol. 81 (1998), p.1977

[9] T. Kawashima, H. Okamoto, H. Yamamoto and A. Kitamura: J. Am. Ceram. Soc. Vol. 99 (1991), p. 1

[10] S. K. Lee, S. Wuttiphan and B. R. Lawn: J. Am. Ceram. Soc. Vol. 80 (1997), p. 2367

[11] S. K. Lee, K. S. Lee, B. R. Lawn and D. K. Kim: J. Am. Ceram. Soc. Vol. 81 (1998), p. 2061

[12] C. H. Hsueh: J. Mater. Sci. Vol. 21 (1986), p. 2067